

1
2
3
4

5
6
7
8

9
10
11
12
13
14
15
16
17
18
19
20
21
22
23
24
25
26

Original Research Article

**MHD Flow of Fluid over a Rotating Inclined
Permeable Plate with Variable Reactive Index**

ABSTRACT

MHD free convection, heat and mass transfer flow over a rotating inclined permeable plate with the influence of magnetic field, thermal radiation and chemical reaction of various order has been investigated numerically. The governing boundary-layer equations are formulated and transformed into a set of similarity equations with the help of similarity variables derived by lie group transformation. The governing equations are solved numerically using the Nactsheim-Swigert Shooting iteration technique together with the Runge-Kutta six order iteration schemes. The simulation results are presented graphically to illustrate influence of magnetic parameter (M), porosity parameter (γ), rotational parameter (R'), Grashof number (G_r), modified Grashof number (G_m), thermal conductivity parameter (T_c), Prandtl number (P_r), radiation parameter (R), heat source parameter (Q), Eckert number (E_c), Schmidt number (S_c), reaction parameter (λ) and order of chemical reaction (n) on the all fluid velocity components, temperature and concentration distribution as well as Skin-friction coefficient, Nusselt and Sherwood number at the plate.

Keywords: MHD; Inclined permeable plate; Thermal radiation; Chemical reaction;

NOMENCLATURE

B_0	Constant magnetic flux density
c	Constant depends on the properties of the fluid
C	Concentration of the fluid
C_p	Specific heat at constant pressure
D_m	Mass diffusivity
f'	Dimensionless primary velocity
g	Acceleration due to gravity
g_0	Dimensionless secondary velocity
k	Thermal conductivity
k_∞	Undisturbed thermal conductivity
k_0	Reaction rate
K	Permeability of the porous medium
n	Order of chemical reaction

27	P	Pressure distribution in the boundary layer
28	q_r	Radiative heat flux in the y direction
29	Q_T	Heat generation
30	Q_0	Heat source
31	t	Time
32	T	Fluid temperature
33	U	Uniform velocity
34	u, v	Velocity components along x and y axes respectively
35	x'	Dimensionless axial distance along x axis
36	Dimensionless parameters	
37	E_c	Eckert number
38	R'	Rotational parameter
39	G_r	Grashof number
40	G_m	Modified Grashof number
41	M	Magnetic parameter
42	P_r	Prandtl number
43	Q	Heat source parameter
44	R	Radiation parameter
45	S_c	Schmidt number
46	T_c	Thermal conductivity parameter
47	γ	Permeability of the porous medium
48	λ	Reaction parameter
49		
50	Greek Symbols	
51	ν	Kinematic viscosity of the fluid
52	μ	Dynamic viscosity of the fluid
53	σ	Electrical conductivity
54	σ_0	Constant electrical conductivity
55	σ_s	Stefan-Boltzmann constant
56	ρ	Density of the fluid
57	α	Thermal diffusivity
58	$\alpha_1 - \alpha_6$	Arbitrary real number

59	β	Inclination angle
60	β_T	Thermal expansion coefficient
61	β_C	Concentration expansion coefficient
62	κ^*	Mean absorption coefficient
63	ε	Parameter of the group
64	ψ	Stream function
65	η	Similarity variable
66	θ	Dimensionless temperature
67	φ	Dimensionless concentration
68	Ω	Angular velocity of the plate
69	Subscripts	
70	w	Condition of the wall
71	∞	Condition of the free steam

72
73
74

1. INTRODUCTION

75 Coupled heat and mass transfer problems in the presence of chemical reactions are of
76 importance in many processes and have, therefore, received considerable amount of
77 attention of researchers in recent years. Chemical reactions can occur in processes such as
78 drying, distribution of temperature and moisture over agricultural fields and groves of fruit
79 trees, damage of crops due to freezing, evaporation at the surface of a water body, energy
80 transfer in a wet cooling tower and flow in a desert cooler. Chemical reactions are classified
81 as either homogeneous or heterogeneous processes. A homogeneous reaction is one that
82 occurs uniformly throughout a given phase. On the other hand, a heterogeneous reaction
83 takes a restricted area or within the boundary of a phase. Analysis of the transport
84 processes and their interaction with chemical reactions is quite difficult and closely related to
85 fluid dynamics. Chemical reaction effects on heat and mass transfer has been analyzed by
86 many researchers over various geometries with various boundary conditions in porous and
87 nonporous media. Symmetry groups or simply symmetries are invariant transformations that
88 do not alter the structural form of the equation under investigation which is described by
89 Bluman and Kumei [1]. MHD boundary layer equations for power law fluids with variable
90 electric conductivity is studied by Helmy [2]. In the case of a scaling group of
91 transformations, the group-invariant solutions are nothing but the well known similarity
92 solutions which is studied by Pakdemirli and Yurusoy [3]. Symmetry groups and similarity
93 solutions for free convective boundary-layer problem was studied by Kalpakides and
94 Balassas [4]. Makinde [5] investigated the effect of free convection flow with thermal
95 radiation and mass transfer past moving vertical porous plate. Seddeek and Salem [6]
96 investigated the Laminar mixed convection adjacent to vertical continuously stretching sheet
97 with variable viscosity and variable thermal diffusivity. Ibrahim, Elaiw and Bakr [7] studied the
98 effect of the chemical reaction and radiation absorption on the unsteady MHD free
99 convection flow past a semi infinite vertical permeable moving plate with heat source and
100 suction. El-Kabeir, El-Hakiem and Rashad [8] studied Lie group analysis of unsteady MHD
101 three dimensional dimensional by natural convection from an inclined stretching surface
102 saturated porous medium. Rajeswari, Jothiram and Nelson [9] studied the effect of chemical

reaction, heat and mass transfer on nonlinear MHD boundary layer flow through a vertical porous surface in the presence of suction. Chandrakala [10] investigated chemical reaction effects on MHD flow past an impulsively started semi-infinite vertical plate. Joneidi, Domairry and Babaelahi [11] studied analytical treatment of MHD free convective flow and mass transfer over a stretching sheet with chemical reaction. Muhaimin, Kandasamy and Hashim [12] studied the effect of chemical reaction, heat and mass transfer on nonlinear boundary layer past a porous shrinking sheet in the presence of suction. Rahman and Salahuddin [13] studied hydromagnetic heat and mass transfer flow over an inclined heated surface with variable viscosity and electric conductivity. As per standard text and works of previous researchers, the radiative flow of an electrically conducting fluid and heat and mass transfer situation arises in many practical applications such as in electrical power generation, astrophysical flows, solar power technology, space vehicle re-entry, nuclear reactors.

The objective of this study is to present a similarity analysis of boundary layer flow past a rotating inclined permeable plate with the influence of magnetic field, thermal radiation, thermal conductivity and chemical reaction of various orders.

2. MATHEMATICAL MODEL OF THE FLOW AND GOVERNING EQUATIONS

Steady two dimensional MHD heat and mass transfer flow with chemical reaction and radiation over an inclined permeable plate $y = 0$ in a rotating system under the influence of transversely applied magnetic field is considered. The x -axis is taken in the upward direction and y -axis is normal to it. Again the plate is inclined at an angle β with the x -axis. The flow takes place at $y \geq 0$, where y is the coordinate measured normal to the x -axis. Initially we consider the plate as well as the fluid is at rest with the same velocity $U (= U_\infty)$, temperature $T (= T_\infty)$ and concentration $C (= C_\infty)$. Also it is assumed that the fluid and plate is at rest after that the whole system is allowed to rotate with a constant angular velocity $R = (0, -\Omega, 0)$ about the y -axis and then the temperature and species concentration of the plate are raised to $T_w (> T_\infty)$ and $C_w (> C_\infty)$ respectively, which are thereafter maintained constant, where T_w and C_w is the temperature and concentration respectively at wall and T_∞ and C_∞ is the temperature and concentration respectively far away from the plate.

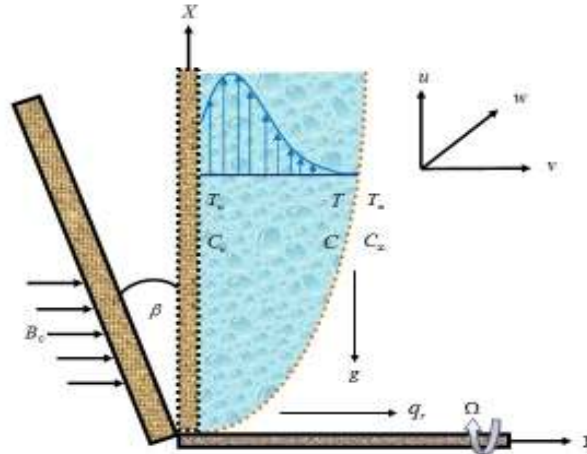


Fig. 1. Physical configuration of the flow

The electrical conductivity is assumed to vary with the velocity of the fluid and have the form [2],

138 $\sigma = \sigma_0 u$, σ_0 is the constant electrical conductivity.

139 The applied magnetic field strength is considered, as follows [13]

140
$$B(x) = \frac{B_0}{\sqrt{x}}$$

141 The temperature dependent thermal conductivity is assumed to vary linearly, as follows [6]

142
$$k(T) = k_\infty [1 + c(T - T_\infty)]$$

143 Where k_∞ is the undisturbed thermal conductivity and c is the constant depending on the
144 properties of the fluid.

145 The governing equations for the continuity, momentum, energy and concentration in laminar
146 MHD incompressible boundary-layer flow is presented follows

147
$$\frac{\partial u}{\partial x} + \frac{\partial v}{\partial y} = 0 \quad (1)$$

148
$$u \frac{\partial u}{\partial x} + v \frac{\partial u}{\partial y} = \nu \frac{\partial^2 u}{\partial y^2} + 2\Omega w - \frac{\nu}{K} u - \frac{\sigma_0 B_0^2 u^2}{\rho x} + g\beta_T (T - T_\infty) \cos\beta + g\beta_C (C - C_\infty) \cos\beta \quad (2)$$

149
$$u \frac{\partial w}{\partial x} + v \frac{\partial w}{\partial y} = \nu \frac{\partial^2 w}{\partial y^2} - 2\Omega u - \frac{\nu}{K} w - \frac{\sigma_0 B_0^2 u w}{\rho x} \quad (3)$$

150
$$u \frac{\partial T}{\partial x} + v \frac{\partial T}{\partial y} = \frac{1}{\rho C_p} \frac{\partial}{\partial y} \left[k(T) \frac{\partial T}{\partial y} \right] + \frac{Q_0 (T - T_\infty)}{\rho C_p} - \frac{\alpha}{k_\infty} \left(\frac{\partial q_r}{\partial y} \right) + \frac{\nu}{C_p} \left(\frac{\partial u}{\partial y} \right)^2 \quad (4)$$

151
$$u \frac{\partial C}{\partial x} + v \frac{\partial C}{\partial y} = D_m \frac{\partial^2 C}{\partial y^2} - k_0 (C - C_\infty)^n \quad (5)$$

152 and the boundary conditions for the model is

153
$$\left. \begin{aligned} u = U, v = 0, w = 0, T = T_w, C = C_w \quad \text{at } y = 0 \\ u \rightarrow 0, w \rightarrow 0, T \rightarrow T_\infty, C \rightarrow C_\infty \quad \text{as } y \rightarrow \infty \end{aligned} \right\} \quad (6)$$

154 where, U is the uniform velocity, β is the inclination angle of the plate with x-axis, C_p is the
155 specific heat at constant pressure, $k(T)$ is the temperature dependent thermal conductivity,
156 Q_0 is the heat source, D_m is the mass diffusivity, k_0 is the reaction rate, $k_0 > 0$ for destructive
157 reaction, $k_0 = 0$ for no reaction and $k_0 < 0$ for generative reaction, n (integer) is the order of
158 chemical reaction, q_r is the chemical reaction parameter, T_w and C_w is the temperature and
159 concentration respectively at wall and T_∞ and C_∞ is the temperature and concentration
160 respectively far away from the plate.

161

162 2.1 METHOD OF SOLUTION

163

164 Introducing the following dimensionless variables

165
$$x' = \frac{xU}{\nu}, y' = \frac{yU}{\nu}, u' = \frac{u}{U}, v' = \frac{v}{U}, w' = \frac{w}{U}, \theta = \frac{T - T_\infty}{T_w - T_\infty} \quad \text{and} \quad \phi = \frac{C - C_\infty}{C_w - C_\infty}$$

166 the following equations are obtained,

167
$$u = U u', v = U v', w = U w', T = T_\infty + (T_w - T_\infty) \theta \quad \text{and} \quad C = C_\infty + (C_w - C_\infty) \phi \quad (7)$$

168 Now, by using equation (7), the equations (1), (2), (3), (4) and (5) are transformed to

169
$$\frac{\partial u'}{\partial x'} + \frac{\partial v'}{\partial y'} = 0 \quad (8)$$

$$u' \frac{\partial u'}{\partial x'} + v' \frac{\partial u'}{\partial y'} = \frac{\partial^2 u'}{\partial y'^2} + 2R'w' - \gamma u' - \frac{Mu'^2}{x'} + G_r \theta \cos \beta + G_m \phi \cos \beta \quad (9)$$

$$u' \frac{\partial w'}{\partial x'} + v' \frac{\partial w'}{\partial y'} = \frac{\partial^2 w'}{\partial y'^2} - 2R'u' - \gamma w' - \frac{Mu'w'}{x'} \quad (10)$$

$$u' \frac{\partial \theta}{\partial x'} + v' \frac{\partial \theta}{\partial y'} - \frac{1}{P_r} \left[(1 + T_c \theta + R) \frac{\partial^2 \theta}{\partial y'^2} + T_c \left(\frac{\partial \theta}{\partial y'} \right)^2 \right] - Q\theta - E_c \left(\frac{\partial u}{\partial y} \right)^2 = 0 \quad (11)$$

$$u' \frac{\partial \phi}{\partial x'} + v' \frac{\partial \phi}{\partial y'} - \frac{1}{S_c} \frac{\partial^2 \phi}{\partial y'^2} + \lambda \phi^n = 0 \quad (12)$$

using equation (7), the boundary condition (6) becomes,

$$\left. \begin{aligned} u' = 1, v' = 0, w' = 0, \theta = 1, \phi = 1 \text{ at } y' = 0 \\ u' \rightarrow 0, w' \rightarrow 0, \theta \rightarrow 0, \phi \rightarrow 0 \text{ as } y' \rightarrow \infty \end{aligned} \right\} \quad (13)$$

where,

$$R' = \frac{\Omega v}{U^2}, \gamma = \frac{v^2}{KU^2}, M = \frac{\sigma_0 B_0^2}{\rho}, G_r = \frac{g \beta_r (T_w - T_\infty) v}{U^3}, G_m = \frac{g \beta_c (C_w - C_\infty) v}{U^3}, T_c = c(T_w - T_\infty),$$

$$R = \frac{16\sigma_s T_\infty^3}{3\kappa^* k_\infty}, P_r = \frac{v}{\alpha}, Q = \frac{Q_0 v}{\rho C_p U^2}, E_c = \frac{U^2}{C_p (T_w - T_\infty)}, S_c = \frac{v}{D_m} \text{ and } \lambda = \frac{k_0 (C_w - C_\infty)^{n-1} v}{U^2}$$

In order to deal with the problem, we introduce the stream function ψ (since the flow is incompressible) defined by

$$u' = \frac{\partial \psi}{\partial y'}, v' = -\frac{\partial \psi}{\partial x'} \quad (14)$$

The mathematical significance of using equation (14) is that the continuity equation (8) is satisfied automatically.

by equation (14), equations (9), (10), (11) and (12) transformed as follows,

$$\frac{\partial \psi}{\partial y'} \frac{\partial^2 \psi}{\partial x' \partial y'} - \frac{\partial \psi}{\partial x'} \frac{\partial^2 \psi}{\partial y'^2} - \frac{\partial^3 \psi}{\partial y'^3} - 2R'w' + \gamma \frac{\partial \psi}{\partial y'} + \frac{M}{x'} \left(\frac{\partial \psi}{\partial y'} \right)^2 - G_r \theta \cos \beta - G_m \phi \cos \beta = 0 \quad (15)$$

$$\frac{\partial \psi}{\partial y'} \frac{\partial w'}{\partial x'} - \frac{\partial \psi}{\partial x'} \frac{\partial w'}{\partial y'} - \frac{\partial^2 w'}{\partial y'^2} + 2R' \frac{\partial \psi}{\partial y'} + \gamma w' + \frac{M}{x'} \frac{\partial \psi}{\partial y'} w' = 0 \quad (16)$$

$$\frac{\partial \psi}{\partial y'} \frac{\partial \theta}{\partial x'} - \frac{\partial \psi}{\partial x'} \frac{\partial \theta}{\partial y'} - \frac{1}{P_r} \left[(1 + T_c \theta + R) \frac{\partial^2 \theta}{\partial y'^2} + T_c \left(\frac{\partial \theta}{\partial y'} \right)^2 \right] - Q\theta - E_c \left(\frac{\partial^2 \psi}{\partial y'^2} \right)^2 = 0 \quad (17)$$

$$\frac{\partial \psi}{\partial y'} \frac{\partial \phi}{\partial x'} - \frac{\partial \psi}{\partial x'} \frac{\partial \phi}{\partial y'} - \frac{1}{S_c} \frac{\partial^2 \phi}{\partial y'^2} + \lambda \phi^n = 0 \quad (18)$$

and the boundary conditions (13) become,

$$\left. \begin{aligned} \frac{\partial \psi}{\partial y'} = 1, \frac{\partial \psi}{\partial x'} = 0, w' = 0, \theta = 1, \phi = 1 \text{ at } y' = 0 \\ \frac{\partial \psi}{\partial y'} \rightarrow 0, w' \rightarrow 0, \theta \rightarrow 0, \phi \rightarrow 0 \text{ as } y' \rightarrow \infty \end{aligned} \right\} \quad (19)$$

Finding the similarity solution of the equations (15) to (18) is equivalent to determining the invariant solutions of these equations under a particular continuous one parameter group. Introducing the simplified form of Lie-group transformations [8] namely, the scaling group of transformations

$$G_1: x^* = x' e^{\mathcal{E} \alpha_1}, y^* = y' e^{\mathcal{E} \alpha_2}, \psi^* = \psi e^{\mathcal{E} \alpha_3}, w^* = w' e^{\mathcal{E} \alpha_4}, \theta^* = \theta e^{\mathcal{E} \alpha_5} \text{ and } \phi^* = \phi e^{\mathcal{E} \alpha_6} \quad (20)$$

Here, $\varepsilon (\neq 0)$ is the parameter of the group and $\alpha's$ are arbitrary real numbers whose interrelationship will be determined by our analysis. Equations (20) may be considered as a point transformation which transforms the coordinates $(x', y', \psi, w', \theta, \varphi)$ to the coordinates $(x^*, y^*, \psi^*, w^*, \theta^*, \varphi^*)$.

The system will remain invariant under the group transformation G_1 , so the following relations among the exponents are obtained from equations (15) to (18),

$$\left. \begin{aligned} \alpha_1 + 2\alpha_2 - 2\alpha_3 &= 3\alpha_2 - \alpha_3 = -\alpha_4 = \alpha_2 - \alpha_3 = -\alpha_5 = -\alpha_6 \\ \alpha_1 + \alpha_2 - \alpha_3 - \alpha_4 &= 2\alpha_2 - \alpha_4 = \alpha_2 - \alpha_3 = -\alpha_4 \\ \alpha_1 + \alpha_2 - \alpha_3 - \alpha_5 &= 2\alpha_2 - \alpha_5 = 2\alpha_2 - 2\alpha_5 = 4\alpha_2 - 2\alpha_3 \\ \alpha_1 + \alpha_2 - \alpha_3 - \alpha_6 &= 2\alpha_2 - \alpha_6 = -n\alpha_6 \end{aligned} \right\} \quad (21)$$

Again, the following relations are obtained from the boundary conditions (19),

$$\left. \begin{aligned} \alpha_2 &= \alpha_3 \\ \alpha_5 &= \alpha_6 = 0 \end{aligned} \right\} \quad (22)$$

Solving the system of linear equations (21) and (22), the following relationship are obtained,

$$\alpha_1 = 2\alpha_2 = 2\alpha_3, \alpha_4 = \alpha_5 = \alpha_6 = 0$$

by using the above relation the equation (20) reduces to the following group of transformation

$$x^* = x' e^{2\varepsilon\alpha_2}, y^* = y' e^{\varepsilon\alpha_2}, \psi^* = \psi e^{\varepsilon\alpha_2}, w^* = w', \theta^* = \theta, \varphi^* = \varphi \quad (23)$$

expanding equation (23) by Taylor's method in powers of ε and keeping terms up to the order ε , we have

$$x^* - x' = 2\varepsilon x' \alpha_2, y^* - y' = \varepsilon y' \alpha_2, \psi^* - \psi = \varepsilon \psi \alpha_2, w^* - w' = 0, \theta^* - \theta = 0, \varphi^* - \varphi = 0$$

In terms of differentials

$$\frac{dx'}{2\alpha_2 x'} = \frac{dy'}{\alpha_2 y'} = \frac{d\psi}{\alpha_2 \psi} = \frac{dw'}{0} = \frac{d\theta}{0} = \frac{d\varphi}{0} \quad (24)$$

Solving the equation (24) the following similarity variables are introduced,

$$\eta = \frac{y'}{\sqrt{x'}}, \psi = \sqrt{x'} f(\eta), w' = g_0(\eta), \theta = \theta(\eta) \text{ and } \varphi = \varphi(\eta)$$

By using the above mentioned variables, equations (15), (16), (17) and (18) becomes

$$f''' + \frac{1}{2} f f'' - M f'^2 + 2R' g_0 - \gamma f' + G_r \theta \cos \beta + G_m \varphi \cos \beta = 0 \quad (25)$$

$$g_0'' + \frac{1}{2} f g_0' - 2R' f' - \gamma g_0 - M f' g_0 = 0 \quad (26)$$

$$\frac{1}{P_r} (1 + T_c \theta + R) \theta'' + \frac{1}{P_r} T_c \theta'^2 + \frac{1}{2} f \theta' + Q \theta + E_c f'^2 = 0 \quad (27)$$

$$\frac{1}{S_c} \varphi'' + \frac{1}{2} f \varphi' - \lambda \varphi^n = 0 \quad (28)$$

The corresponding boundary conditions (19) become

$$\left. \begin{aligned} f' &= 1, f = 0, g_0 = 0, \theta = 1, \varphi = 1 \text{ at } \eta = 0 \\ f' &\rightarrow 0, g_0 \rightarrow 0, \theta \rightarrow 0, \varphi \rightarrow 0 \text{ as } \eta \rightarrow \infty \end{aligned} \right\} \quad (29)$$

where primes denote differentiation with respect to η only and the parameters are defined as

$$M = \frac{\sigma_0 B_0^2}{\rho} \text{ is the magnetic parameter,}$$

226 $\gamma = \frac{v^2 x'}{KU^2}$ is the porosity parameter

227 $R' = \frac{\Omega v x'}{U^2}$ is the rotational parameter

228 $G_r = \frac{g \beta_T (T_w - T_\infty) v x'}{U^3}$ is the Grashof number

229 $G_m = \frac{g \beta_c (C_w - C_\infty) v x'}{U^3}$ is the modified Grashof number

230 $T_c = c(T_w - T_\infty)$ is the thermal conductivity parameter

231 $P_r = \frac{v}{\alpha}$ is the Prandtl number

232 $R = \frac{16 \sigma_s T_\infty^3}{3 \kappa^* k_\infty}$ is the radiation parameter

233 $Q = \frac{Q_0 v}{\rho C_p U^2}$ is the heat source parameter

234 $E_c = \frac{U^2}{C_p (T_w - T_\infty)}$ is Eckert number

235 $S_c = \frac{v}{D_m}$ is the Schmidt number

236 $\lambda = \frac{k_0 (C_w - C_\infty)^{n-1} v}{U^2}$ is the reaction parameter

237 and n (integer) is the order of chemical reaction

238

239 **2.2 SKIN-FRICTION COEFFICIENTS, NUSSELT AND SHERWOOD NUMBER**

240

241 The physical quantities of the skin-friction coefficients, the reduced Nusselt number and
242 reduced Sherwood number are calculated respectively by the following equations,

243 $C_f (R_e)^{\frac{1}{2}} = -f''(0)$ (30)

244 $C_{g_0} (R_e)^{\frac{1}{2}} = -g'_0(0)$ (31)

245 $N_u (R_e)^{-\frac{1}{2}} = -\theta'(0)$ (32)

246 $S_h (R_e)^{-\frac{1}{2}} = -\phi'(0)$ (33)

247 where, $R_e = \frac{U x'}{v}$ is the Reynolds number.

248

249 **3. RESULTS AND DISCUSSION**

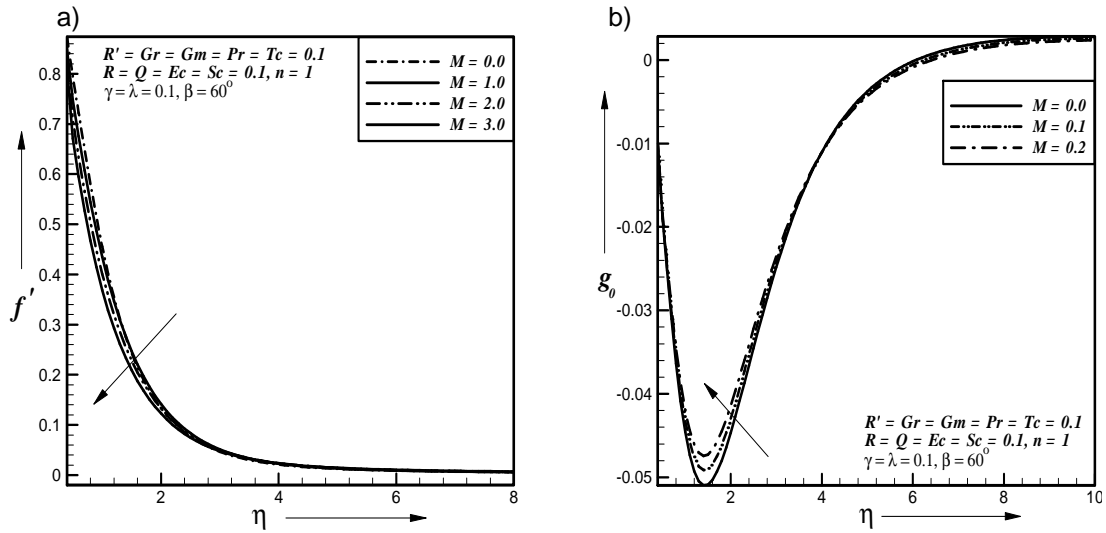
250

251 Heat and mass transfer problem associated with laminar flow past an inclined plate of a
252 rotating system are studied in this work. In order to investigate the physical representation
253 of the problem, the numerical values of primary velocity, secondary velocity, temperature
254 and species concentration from equations (25), (26), (27) and (28) with the boundary layer
255 have been computed for different parameters as the magnetic parameter (M), the rotational

parameter (R'), the porosity parameter (γ), the Grashof number (G_r), the modified Grashof number (G_m), the radiation parameter (R), the Prandtl number (Pr), the Eckert number (Ec), the thermal conductivity parameter (T_c), the heat source parameter (Q), the Schmidt number (Sc), the reaction parameter (λ), the inclination angle (β) and the order of chemical reaction (n) respectively.

Figs. 2a and 2b show that with the increases of magnetic parameter, primary velocity profiles decreases but secondary velocity profiles increases. Figs. 3a-3d represents that with the increase of rotational parameter, primary velocity decreases but secondary velocity, temperature and concentration profiles increases.

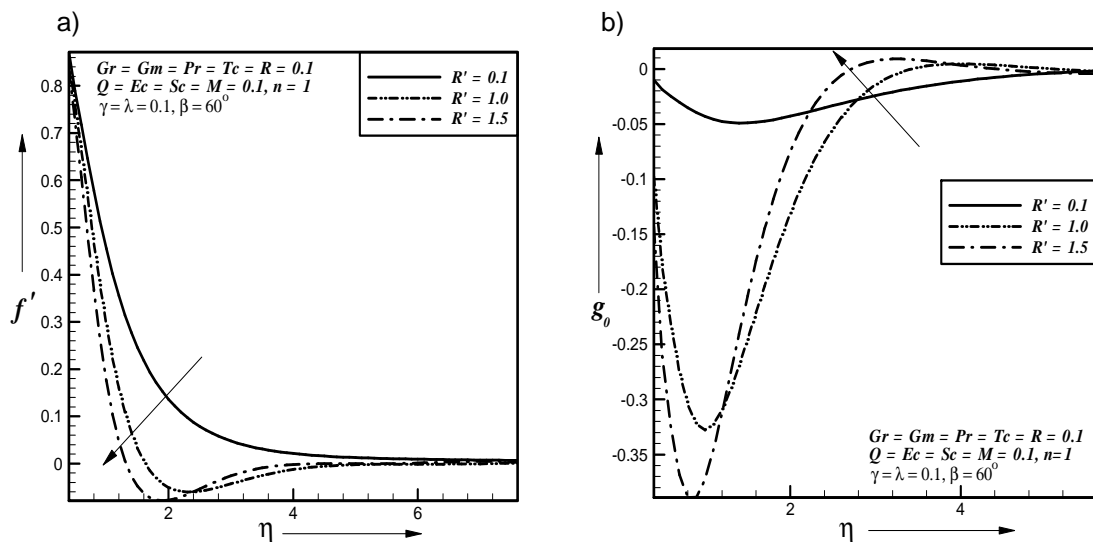
265
266



267
268

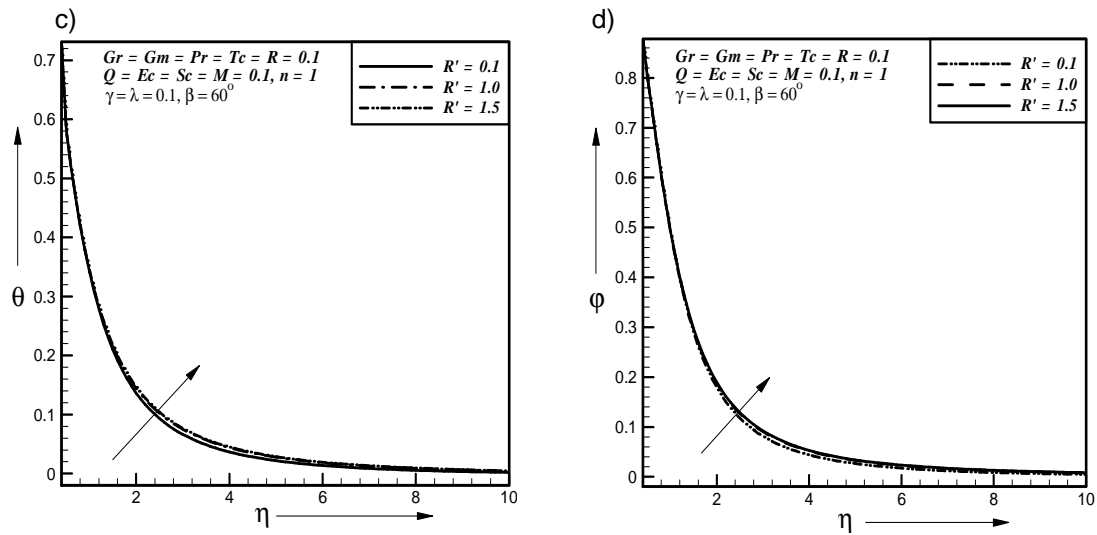
269 **Fig. 2. Effect of magnetic parameter on a) primary velocity b) secondary velocity**
270 **profiles**

271
272
273
274



275

276
277



278
279

Fig. 3. Effect of rotational parameter on a) primary velocity b) secondary velocity c) temperature d) concentration profiles

280

In Figs. 4a-4d, primary velocity profiles decreases but the secondary velocity, temperature and concentration profiles increases with the increase of porosity parameter. With the increase of inclination angle, primary velocity profiles decreases but secondary velocity profiles increases(Figs. 5a and 5b).

281

In Figs. 6a-6c, we see that with the increase of Grashof number, primary velocity profiles increases but secondary velocity and temperature profiles decreases. Figs. 7a- 7c show that with the increase of modified Grashof number, primary velocity profiles increases but secondary velocity and concentration profiles decreases. With the increase of Prandtl number, primary velocity profiles increases but temperature decreases (Figs. 8a and 8b).

282

283

284

285

286

287

288

289

290

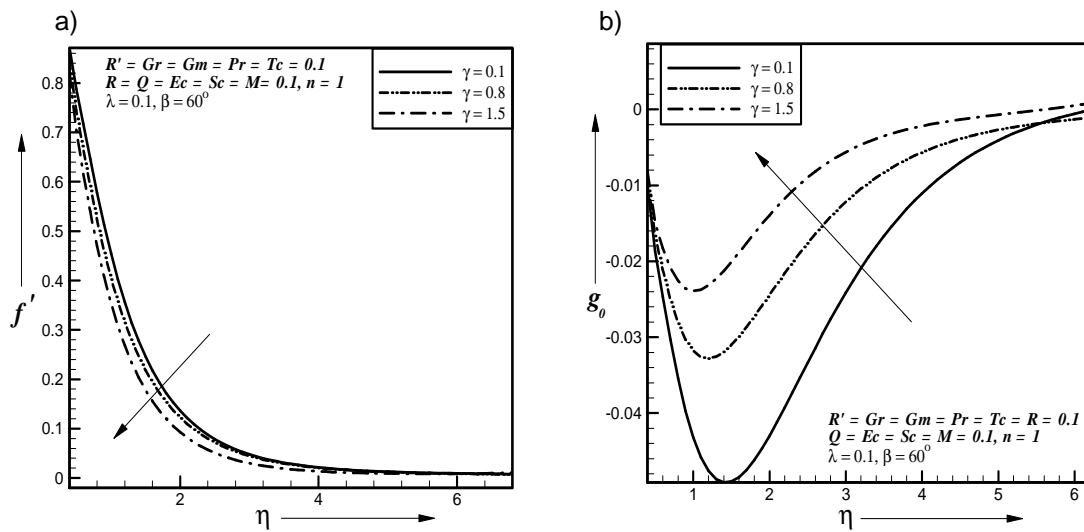
291

292

293

294

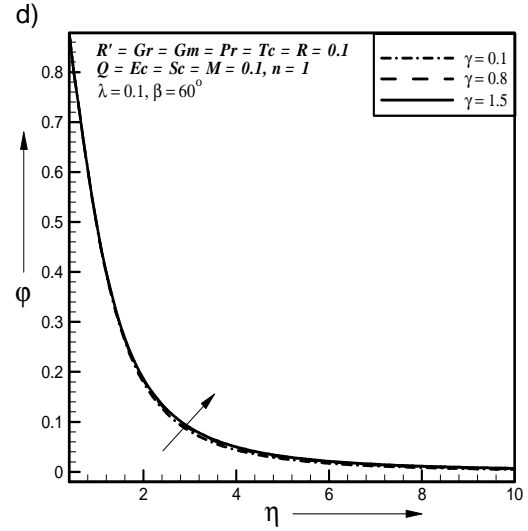
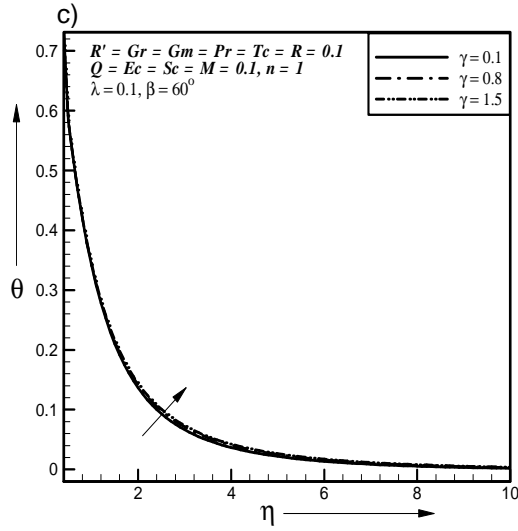
295



296

297

298



299

300

301

302

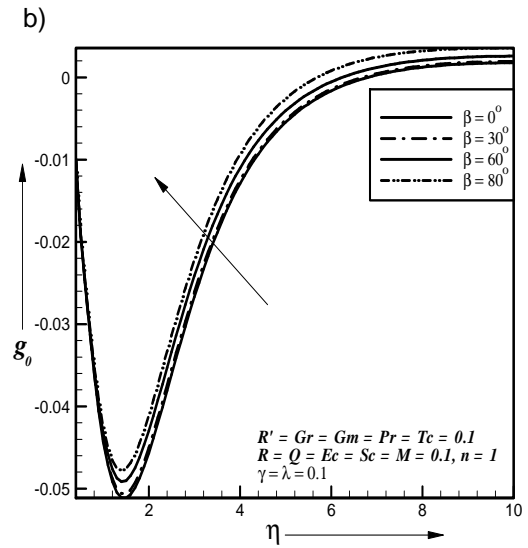
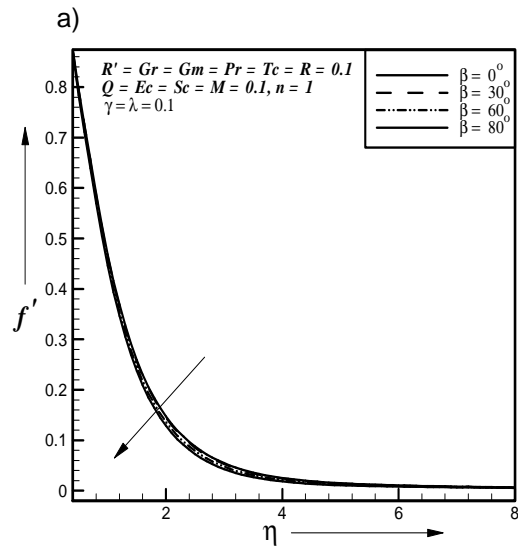
303

304

305

306

Fig. 4. Effect of porosity parameter γ on a) primary velocity b) secondary velocity c) temperature d) concentration profiles



307

308

309

310

311

312

313

314

315

316

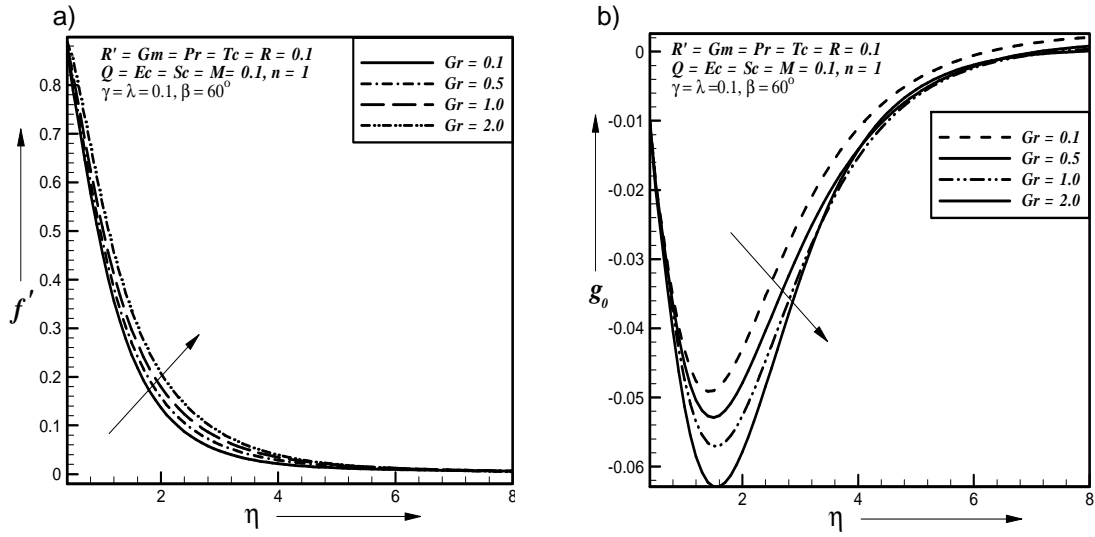
317

318

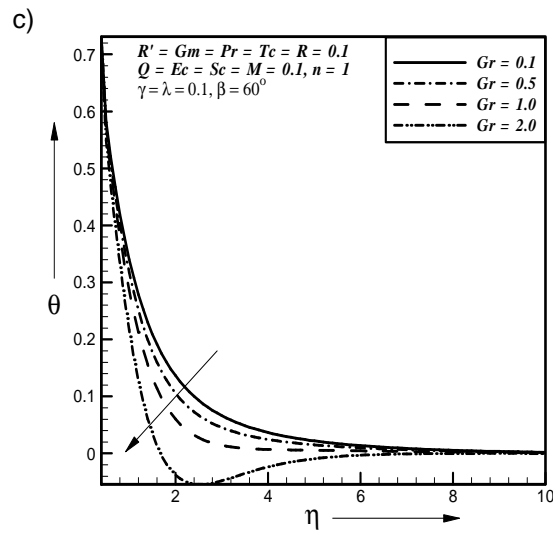
319

Fig. 5. Effect of inclination angle on a) primary velocity b) secondary velocity profiles

320



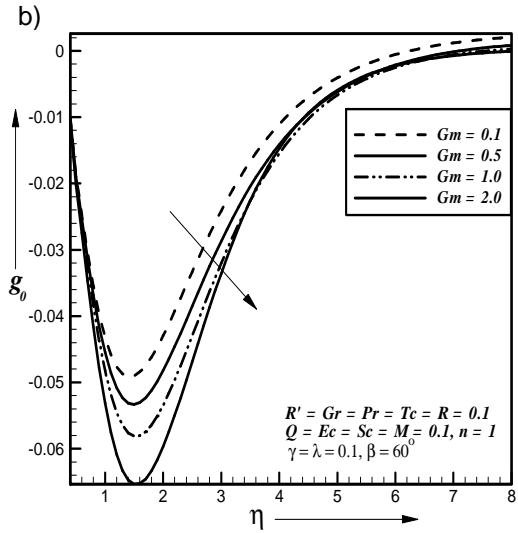
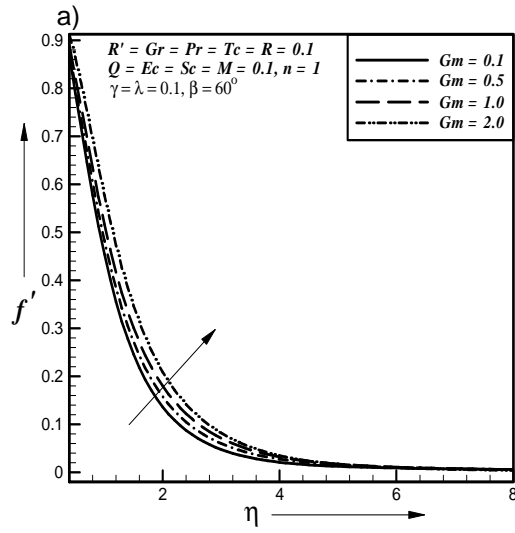
321
322
323
324
325
326



327
328
329
330
331
332
333
334
335
336
337
338
339
340
341
342

Fig. 6. Effect of Grashof number on a) primary velocity b) secondary velocity c) temperature profiles

343



344

345

346

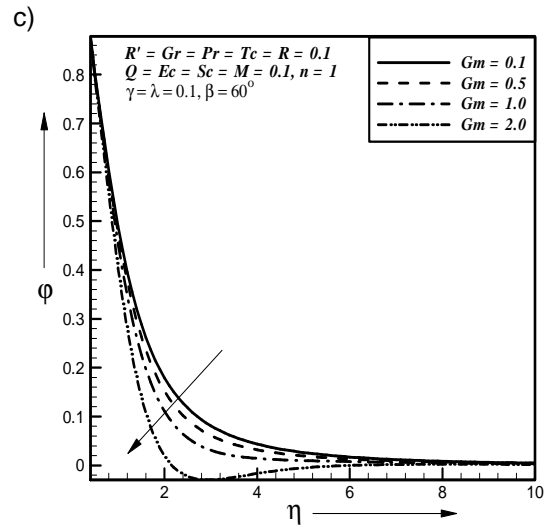
347

348

349

350

351



352

353

354

355

356

357

358

359

360

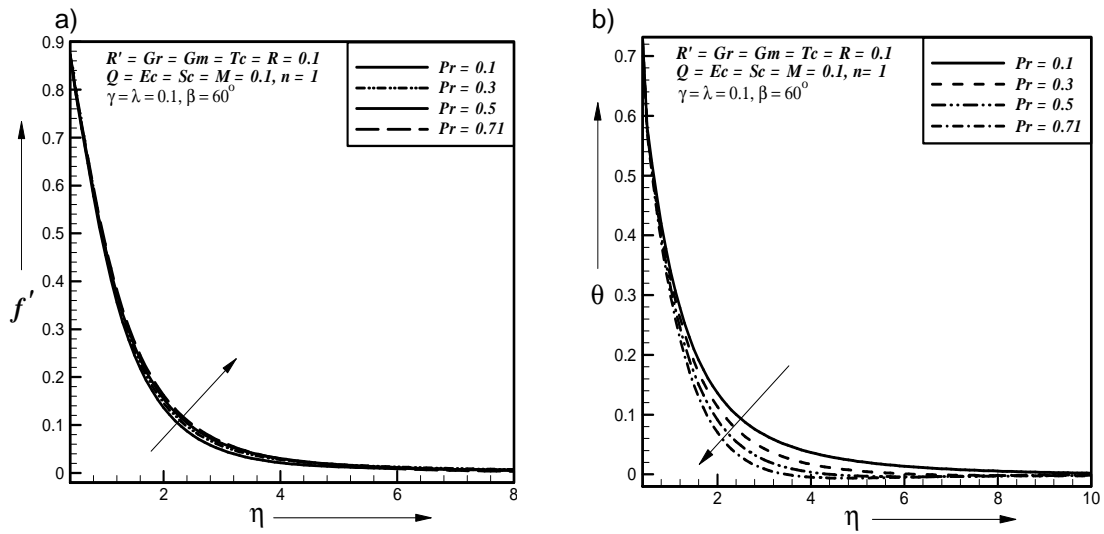
361

362

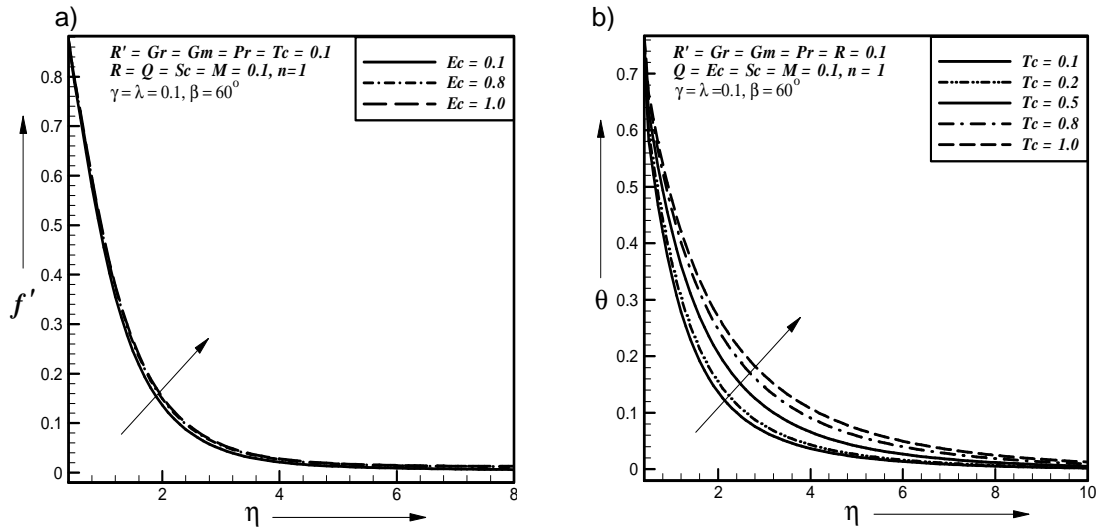
363

Fig. 7. Effect of modified Grashof number on a) primary velocity b) secondary velocity c) concentration profiles

364 Fig. 9a, It is observe that the primary velocity profile increases with the increase of Eckert
 365 number. In Fig. 9b, temperature profile increases with the increase of Thermal conductivity
 366 parameter.
 367
 368



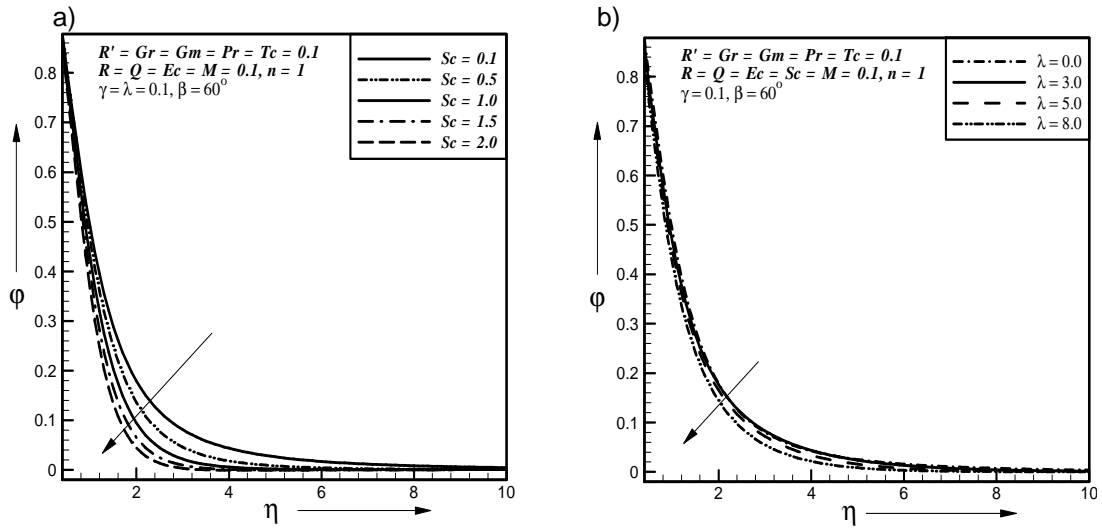
369
 370
 371 **Fig. 8. Effect of Prandtl number on a) primary velocity b) temperature profiles**
 372
 373
 374
 375
 376
 377



378
 379
 380 **Fig. 9. Effect of a) Eckert number on primary velocity profiles b) thermal conductivity**
 381 **parameter on temperature profiles**
 382

383 In Fig. 10a, concentration profiles decreases with the increase of Schmidt number. Fig. 10b
 384 represents no reaction ($\lambda = 0.0$) and destructive reaction ($\lambda > 0.0$), where the concentration
 385 profiles decreases with the increase of reaction parameter.

386
387



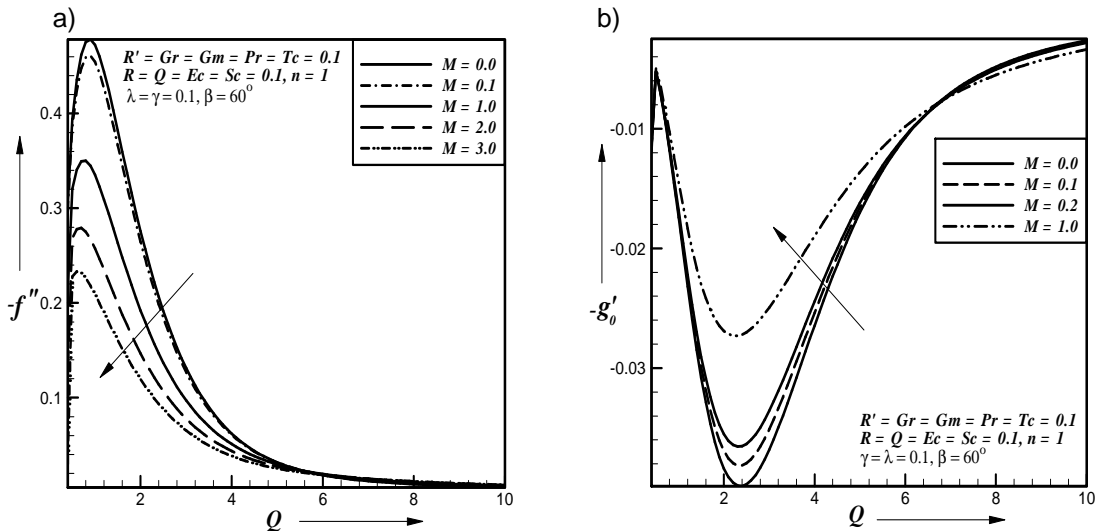
388
389
390
391

Fig. 10. Effect of a) Schmidt number on concentration profiles b) reaction parameter on concentration profiles

392 For the physical interest of the problem, the dimensionless skin-friction coefficient ($-f''$)
393 ($-g'_0$), the dimensionless heat transfer rate ($-\theta'$) and the dimensionless mass transfer rate
394 ($-\phi'$) at the plate are plotted against Heat source parameter (Q) and illustrated in Figs. 11-
395 19.

396 In Figs. 11a-11b and 12a-12b, primary shear stress decreases but secondary shear stress
397 increases with the increase of magnetic parameter and heat source parameter (Q)
398 respectively.

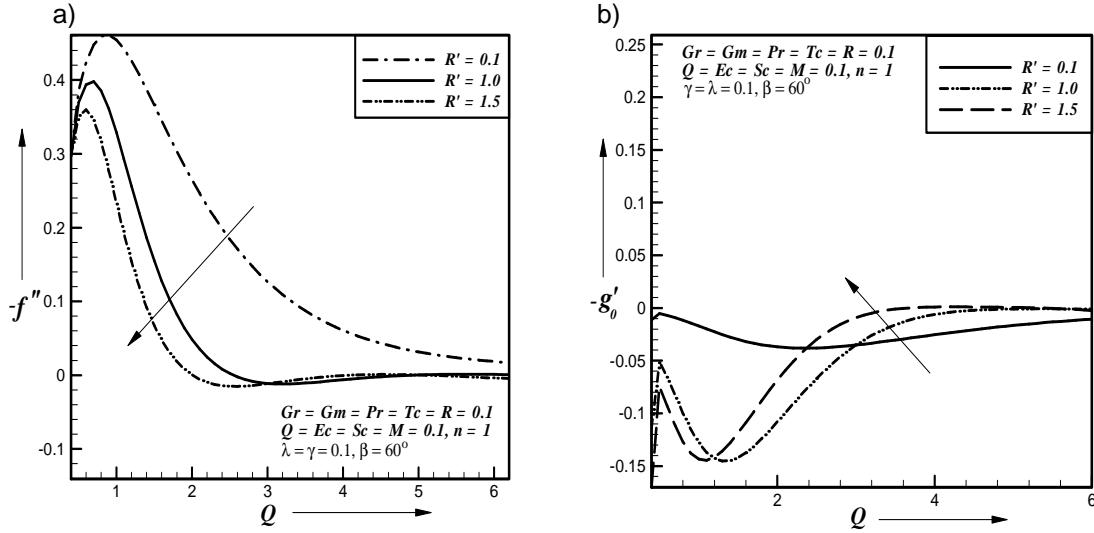
399
400



401
402
403
404
405

Fig. 11. Effect of magnetic parameter on a) primary shear stress b) secondary shear stress

406



407

408

409 **Fig. 12. Effect of rotational parameter on a) primary shear stress b) secondary shear**
 410 **stress**

411

412 Figs. 13a and 13b represent that primary shear stress decreases but secondary shear stress
 413 increases with the increase of porosity parameter.

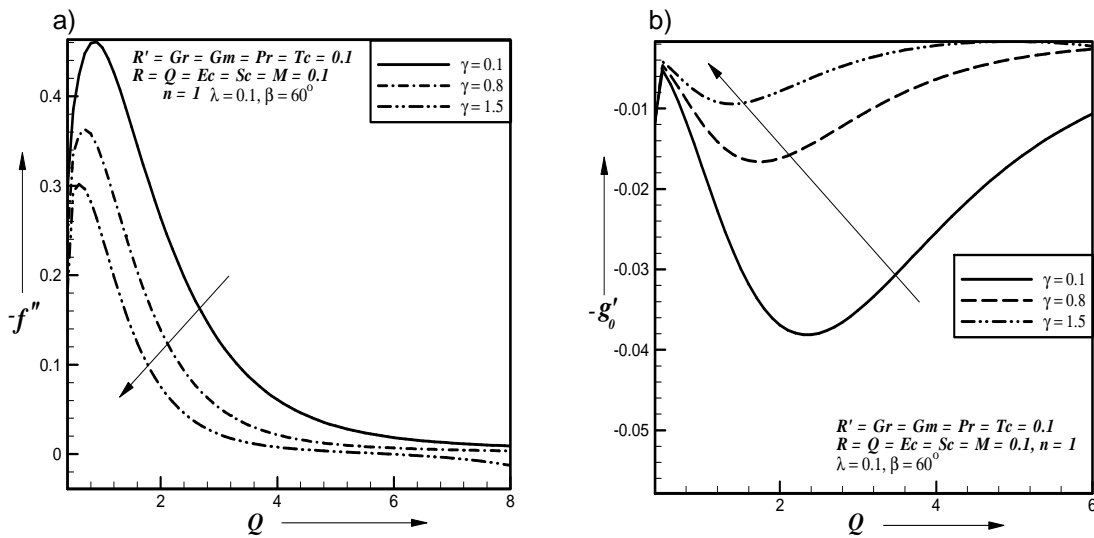
414

415

416

417

418



419

420

421 **Fig. 13. Effect of porosity parameter on a) primary b) secondary shear stress**

422

423 In Fig. 14a and Fig. 14b, primary shear stress increases with the increase of Grashof
 424 number and modified Grashof number respectively.

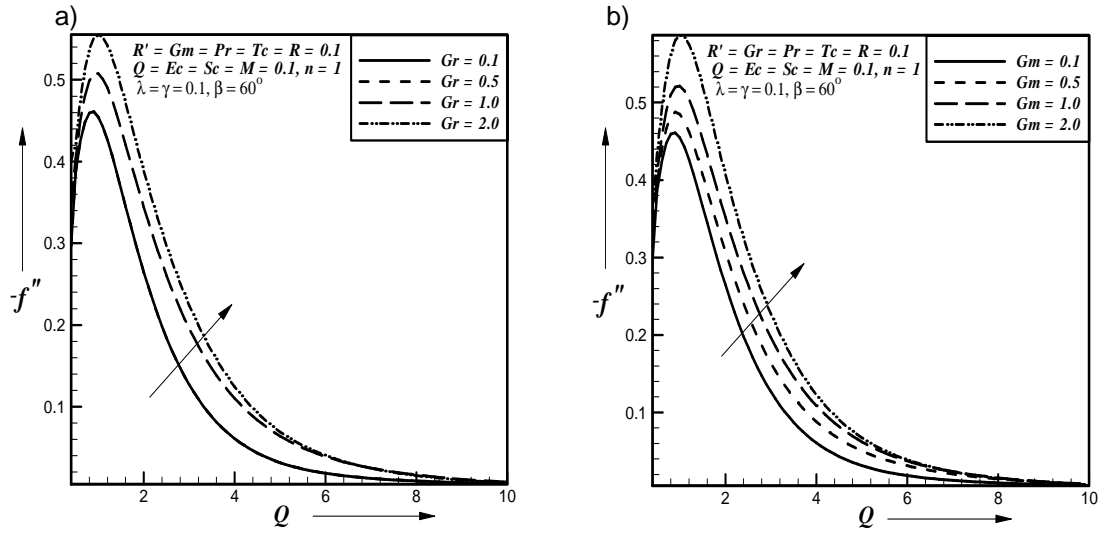
425

426

427

428

429



430

431

432

433

434

435

436

437

438

439

440

441

442

443

444

Fig. 14. Effect of a) Grashof number b) modified Grashof on primary shear stress

In Fig. 15a, primary shear stress decreases with the increase of inclination angle. In Fig. 15b, the heat transfer rate increases with the increase of thermal conductivity parameter. Fig. 16a, the heat transfer rate decreases with the increase of Prandtl number. Fig. 16b, the heat transfer rate increases with the increase of heat source parameter.

445

446

447

448

449

450

451

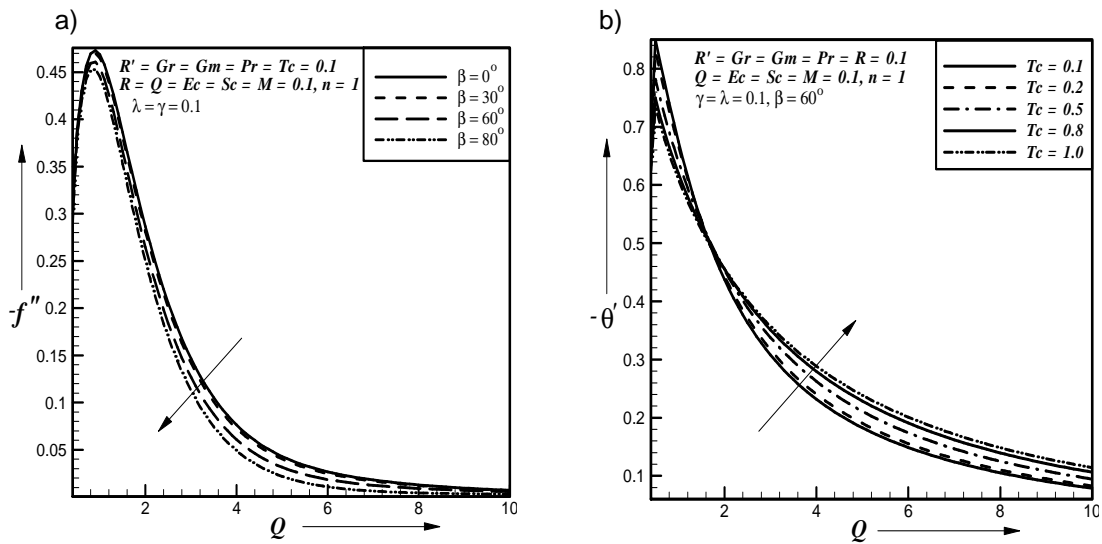
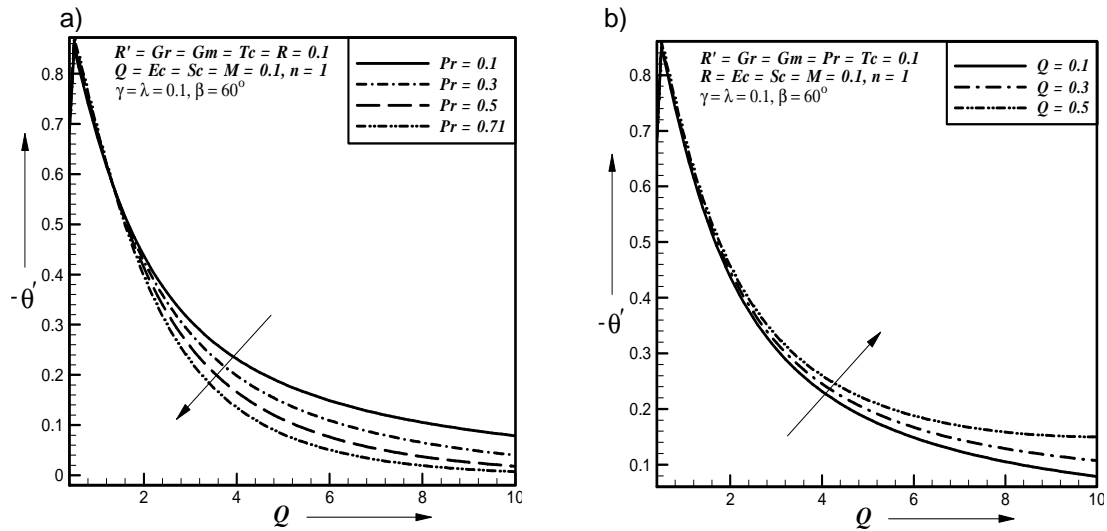


Fig. 15. Effect of a) inclination angle on primary shear stress b) thermal conductivity parameter on heat transfer rate

452



453

454

455

456

457

458

459

460

461

462

463

464

465

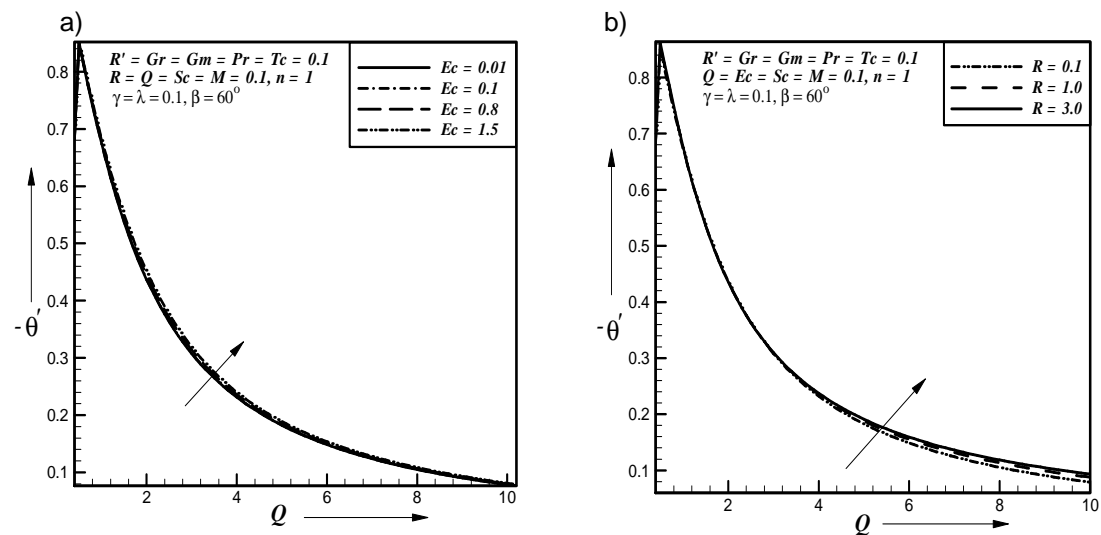
466

467

468

Fig. 16. Effect of a) Prandtl number b) heat source parameter on heat transfer rate

In Fig. 17a -17b, the heat transfer rate increases with the increase of Eckert number and radiation parameter. Fig. 18a -Fig. 18b, the mass transfer rate decreases with the increase of Schmidt number and reaction parameter. Fig. 19 represents that the mass transfer rate increases with the increase of order of chemical reaction parameter.



469

470

471

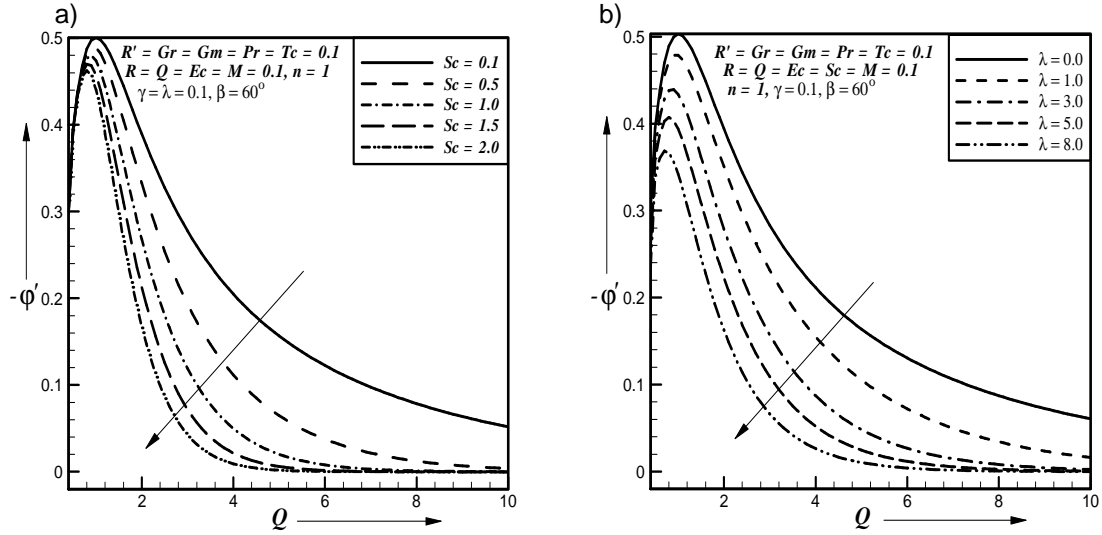
472

473

474

Fig. 17. Effect of a) Eckert number b) radiation parameter on heat transfer rate

475



476

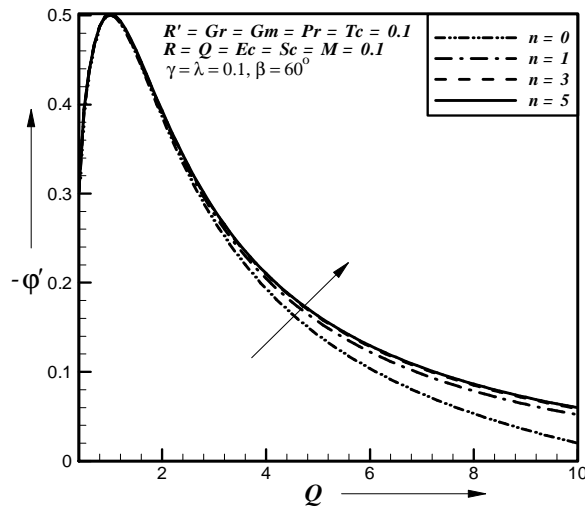
477

478

479

480

Fig. 18. Effect of a) Schmidt number b) reaction parameter on mass transfer rate



481

482

483

484

485

486

Fig. 19. Effect of order of chemical reaction on mass transfer rate

4. CONCLUSION

487

488

489

490

491

492

493

494

495

Primary velocity profiles decreases and primary shear stress with the increase of magnetic parameter, rotational parameter, but reverse effect is found for the secondary velocity profiles and secondary shear stress. Primary shear stress decreases due to increase of magnetic parameter where as the reverse effect is found for secondary shear stress. Temperature and concentration boundary layer thickness increases due to increase of rotational parameter. The primary velocity profiles and primary shear stress decreases due to increase of permeability of the porous medium and inclination angle but reverse effect is found for the secondary velocity profiles and secondary shear stress. Temperature and concentration

boundary layer thickness are increases due to increase of permeability of the porous medium.

The primary velocity profiles and primary shear stress increases due to increase of Grashof number where as the reverse effect is found for the secondary velocity profiles. Also the temperature boundary layer thickness is decreases due to increase of Grashof number.

The primary velocity profiles and primary shear stress increases due to increase of modified Grashof number where as the reverse effect is found for the secondary velocity profiles. Also the concentration boundary layer thickness decreases due to increase of modified Grashof number.

The primary velocity profiles increases due to increase of Prandtl number. The thermal boundary layer thickness as well as the heat transfer rate at the plate decreases as the Prandtl number increases.

The heat transfer rate at the plate as well as the primary velocity is increases due to increase of Eckert number and thermal conductivity parameter.

The heat transfer rate at the plate increases due to increase of heat source parameter and radiation parameter.

The concentration boundary layer thickness as well as the mass transfer rate at the plate decreases due to increase of Schmidt number, no reaction and destructive reaction.

The mass transfer rate at the plate increases due to increase of order of chemical reaction.

515

516 **COMPETING INTERESTS**

517

518 Authors have declared that no competing interests exist.

519

520

521 **REFERENCES**

522

- 523 1. Bluman GW, Kumei S. Symmetries and Differential Equations. Springer-verlag: New
524 York; 1989.
- 525 2. Helmy KA. MHD boundary layer equations for power law fluids with variable electric
526 conductivity. *Mechanica*. 1995;30:187-200.
- 527 3. Pakdemirli M, Yurusoy M. Similarity transformations for partial differential equations.
528 *SIAM Review*. 1998;40:96-101.
- 529 4. Kalpakides VK, Balassas KB. Symmetry groups and similarity solutions for a free
530 convective boundary-layer problem. *International Journal of Non-Linear Mechanics*.
531 2004;39:1659-1670.
- 532 5. Makinde OD. Free convection flow with thermal radiation and mass transfer past moving
533 vertical porous plate. *International Communications in Heat and Mass Transfer*. 2005 ;
534 32:1411-1419.
- 535 6. Seddeek MA, Salem AM. Laminar mixed convection adjacent to vertical continuously
536 stretching sheet with variable viscosity and variable thermal diffusivity. *Heat and Mass
537 Transfer*. 2005;41:1048-1055.
- 538 7. Ibrahim FS, Elaiw AM, Bakr AA. Effect of the chemical reaction and radiation absorption
539 on the unsteady MHD free convection flow past a semi infinite vertical permeable
540 moving plate with heat source and suction. *Communications in Nonlinear Science and
541 Numerical Simulation*. 2008; 13:1056-1066.
- 542 8. El-Kabeir SMM, El-Hakiem MA, Rashad. Lie group analysis of unsteady MHD three
543 dimensional dimensional by natural convection from an inclined stretching surface
544 saturated porous medium. *Journal of Computational and Applied Mathematics*.
545 2008;213:582-603.

- 546 9. Rajeswari R, Jothiram J, Nelson VK. Chemical Reaction, Heat and Mass Transfer on
547 Nonlinear MHD Boundary Layer Flow through a Vertical Porous Surface in the Presence
548 of Suction. *Applied Mathematical Sciences*. 2009;3:2469-2480.
- 549 10. Chandrakala P. Chemical Reaction Effects on MHD Flow Past An Impuissively Started
550 Semi-Infinite Vertical Plate. *International Journal of Dynamics of Fluids*. 2010;6:77-79.
- 551 11. Joneidi AA, Domairry G, Balaehi M. Analytical treatment of MHD free convective flow
552 and mass transfer over a stretching sheet with chemical reaction. *Journal of the Taiwan*
553 *Institute of Chemical Engineers*. 2010;41: 35-43.
- 554 12. Muhaimin, Kandasamy R, Hashim I. Effect of chemical reaction, heat and mass transfer
555 on nonlinear boundary layer past a porous shrinking sheet in the presence of suction.
556 *Nuclear Engineering and Design*. 2010;240(5):933-939.
- 557 13. Rahman MM, Salahuddin KM. Study of hydromagnetic heat and mass transfer flow over
558 an inclined heated surface with variable viscosity and electric conductivity.
559 *Communications in Nonlinear Science and Numerical Simulation*. 2010;15:2073-2085.